

BASIC SCIENCE ARTICLE


CPAP-induced airway hyper-reactivity in mice is modulated by hyaluronan synthase-3

Catherine A. Mayer¹, Abhrajit Ganguly¹, Aubrey Mayer¹, Christina M. Pabelick^{2,3}, Y. S. Prakash^{2,3}, Vince C. Hascall⁴, Ron J. Midura⁴, Valbona Cali⁴, Christopher A. Flask⁵, Bernadette O. Erokwu⁵, Richard J. Martin¹ and Peter M. MacFarlane¹✉

© The Author(s), under exclusive licence to the International Pediatric Research Foundation, Inc 2021

BACKGROUND: Continuous positive airway pressure (CPAP) is a primary mode of respiratory support for preterm infants. Animal studies have shown long-term detrimental effects on lung/airway development, particularly airway (AW) hyper-reactivity, as an unfortunate consequence of neonatal CPAP. Since the hyaluronan (HA) synthesizing enzyme hyaluronan synthase-3 (HAS3) is involved in various adult pulmonary disorders, the present study used a neonatal mouse model to investigate the role of HAS3 in CPAP-induced AW hyper-reactivity.

METHODS: Male and female neonatal mice were fitted with a custom-made mask for delivery of daily CPAP 3 h/day for 7 days. At postnatal day 21 (2 weeks after CPAP ended), airway (AW) hyper-reactivity and HAS3 expression were assessed with and without in vitro HAS3 siRNA treatment.

RESULTS: MRIs of 3-day-old mice confirmed that CPAP increased lung volume with incrementing inflation pressures. CPAP increased AW reactivity in both male and female mice, which was associated with increased airway smooth muscle and epithelial HAS3 immunoreactivity. CPAP did not affect HA accumulation, but HAS3 siRNA reversed CPAP-induced AW hyper-reactivity and reduced HAS3 expression.

CONCLUSIONS: These data in mice implicate a role for HAS3 in long-term effects of CPAP in the developing airway in the context of preterm birth and CPAP therapy.

Pediatric Research (2022) 92:685–693; <https://doi.org/10.1038/s41390-021-01695-0>

IMPACT:

- Neonatal CPAP increases airway smooth muscle and epithelial HAS3 expression in mice.
- CPAP-induced airway hyper-reactivity is modulated by HAS3.
- These data enhance our understanding of the role mechanical forces play on lung development.
- These data are a significance step toward understanding CPAP effects on developing airway.
- These data may impact clinical recognition of the ways that CPAP may contribute to wheezing disorders of former preterm infants.

INTRODUCTION

Airway (AW) hyper-reactivity associated with asthma and wheezing disorders represent major long-term respiratory morbidities of former preterm infants.^{1–3} Supplemental O₂ and continuous positive airway pressure (CPAP) have become the primary modes of respiratory support for preterm infants with respiratory distress.^{3,4} While clinical practice has shifted towards moderate O₂ levels that has reduced lung parenchymal damage, supplemental O₂ therapy is considered a major contributor to the pathogenesis of AW hyper-reactivity, which has been corroborated by numerous animal studies.^{5–9} The use of CPAP is certainly beneficial for early alveolar development, but the long-term effects beyond the period of CPAP administration are not clear.

Using a mouse model, we showed previously that a week of neonatal CPAP (delivered daily to unanesthetized mice) causes a long-term (weeks) increase in AW reactivity beyond the CPAP period.¹⁰ Thus, it is possible that although CPAP is beneficial in the context of alveolar expansion and lung growth in prematurity, there may be detrimental long-term effects on the bronchial AW. What is less clear are the underlying mechanisms by which CPAP effects may occur in the developing AW.

While a number of mechanisms could contribute to CPAP/stretch effects in the premature AW, there is increasing interest in interactions between extracellular matrix (ECM) components and AW cells in mediating and modulating structure and function.^{11–14} Emerging data in adult AW research suggest a role for hyaluronan

¹Department of Pediatrics, Division of Neonatology, Rainbow Babies & Children's Hospital, Case Western Reserve University, Cleveland, OH, USA. ²Department of Anesthesiology and Perioperative Medicine, Mayo Clinic, Rochester, MN, USA. ³Department of Physiology and Biomedical Engineering, Mayo Clinic, Rochester, MN, USA. ⁴Department of Biomedical Engineering, Cleveland Clinic Lerner Research Institute, Cleveland, OH, USA. ⁵Department of Biomedical Engineering, Case Western Reserve University, Cleveland, OH, USA. ✉email: pmm71@case.edu

(HA), a major ECM component composed of repeating disaccharides of D-glucuronic acid and N-acetyl-D-glucosamine.^{13–15} Three synthase isoforms (HAS1, HAS2, and HAS3) synthesize HA, and these enzymes are in part distinguishable by the molecular weight (MW) of HA they synthesize.¹¹ HAS1 and HAS2 synthesize high MW HA (HA^{HMW}; >500 kDa), which has anti-inflammatory properties whereas HAS3 synthesizes the smaller pro-inflammatory and pro-proliferative low MW HA (HA^{LMW}; <500 kDa).^{11,12,14,16} Conversely, a number of hyaluronidases (HYALs) degrade HA,^{12,14} which can lead to HA^{LMW} signaling of downstream effectors, including activation of receptors such as CD44, TLR4, inter- α -inhibitor (I α) as well as inflammatory pathways. Although HA synthesis, degradation, and signaling are not entirely understood in the AW, increased HA^{LMW} has been associated with lung injury,^{17,18} COPD,¹⁹ asthma,^{20,21} and pulmonary fibrosis.^{18,22} Less is known regarding HA in the developing lung. Preterm infants who died within 8 months of birth exhibited significantly higher pleural HA expression, with even higher expression in infants exposed to intrauterine infection.²³ In premature rabbits, hyperoxia increases lung HA expression,²⁴ and in premature primates, increased lung HA deposition was associated with severity of respiratory distress and duration of mechanical ventilation.²⁵ Mechanical ventilation also increased pleural liquid HA expression in adult rabbits^{26,27} whereas in adult mice, mechanical ventilation and subsequent lung injury was associated with increased HA^{LMW} and HAS3 mRNA, which was not observed in HAS3 KO mice.^{17,28,29} Collectively, these data suggest that altered HA function could be promoted by pulmonary distension during the neonatal period in the developing lung. Whether such effects are relevant to bronchial AW is unknown. Significance lies in the potential for the static intraluminal stretch of CPAP superimposed on the mechanical forces of oscillatory breathing transferred to the bronchial AW via tethered parenchyma in the context of CPAP administration in prematurity. In the present study, therefore, we tested the hypothesis that the long-term (weeks) increase in AW reactivity following neonatal CPAP in mice is associated with increased AW HAS3 expression and HA synthesis, and whether these effects of CPAP can be reversed by inhibiting HAS3.

METHODS

Subjects

Time-pregnant mice (C57BL/6J) were purchased from a commercial vendor (Charles River, Wilmington, MA). The day after birth (P1), both male and female mouse pups were randomized to be treated with or without CPAP (in 21% O₂) for the first week of postnatal life as described previously,¹⁰ i.e. until P7. Two weeks after CPAP ended (P7), mice were euthanized and the lungs prepared for: (1) measurements of AW reactivity using the precision lung slice preparation method;¹⁰ (2) reverse transcription PCR (qRT-PCR) for changes in whole-lung gene expression; (3) immunohistochemical analysis of HAS3 and α SM-actin expression; (4) lung HA accumulation; and (5) interference of HAS3 using siRNA. All procedures were carried out in accordance with the National Institute of Health (NIH) guidelines for care and use of laboratory animals and were approved by the Animal Care and Use Committee at Case Western Reserve University.

Neonatal CPAP

Following the day of birth (P0), the litter was divided in half, and both male and female pups were randomly assigned to receive one of four levels of CPAP (0 (control), 1, 3, or 6 cm H₂O) starting the following day (P1) for the first seven postnatal days as previously described.^{10,30} The pups and the dam were maintained in a temperature-controlled room during a 12:12 h, light:dark cycle and provided food and water ad lib.

The details of the neonatal CPAP apparatus and technique have been previously published.¹⁰ Briefly, each day mice were separate from the dam and fitted with a custom-made mask to administer CPAP while resting on a temperature-controlled heat pad (Gaymar T/pump, Orchard Park, NY). Animals were unanesthetized and spontaneously breathing. The mask was designed with an entry port into the mask to deliver humidified air, which passed through to an exit port connected to a downstream manometer. An adjustable leak in the tubing between mask and manometer enabled

continuous flow through the mask, while also allowing fine adjustment of the back-pressure to the mask and thus, to achieve a desired level of CPAP (see S1). A custom-made system allowed delivery of CPAP to multiple mice simultaneously. CPAP was administered for 2 h on the first day to minimize the duration the pups were separated from the mother, but was increased to 3 h/session for the following six consecutive days (7 days total). Control mice were also separated from the dam, and underwent the same procedures of mask fitting, heat pad, and identical airflow, but did not receive CPAP (i.e. 0 cm H₂O). After each session of CPAP, the mask was removed, and the pups were returned to the mother to resume normal rearing. For any one animal, the same level of CPAP was repeated daily for seven consecutive days from P1 through P7.

At the end of the 7 days of CPAP, the mice were allowed an additional 2 weeks of un-interrupted maternal care at which time the pups were prepared for assessment of AW reactivity to methacholine challenge using the in vitro precision-cut living lung slice preparation. Additional mice were used for rPCR on whole-lung homogenates, HA expression using fluorophore-assisted carbohydrate electrophoresis (FACE), and also thin sections for immunohistochemistry.

Precision lung slice preparation and measurements of AW reactivity

The lung slice technique has also been previously described.¹⁰ At P21 (2 weeks after CPAP treatment ended), mice were sacrificed via anesthetic overdose (intraperitoneal injection of a ketamine/xylazine mix, 100 mg/kg/10 mg/kg, respectively) and prepared for in vitro measurements of AW reactivity to methacholine using the lung slice method. To prepare slices, the mouse was placed supine, the trachea cannulated (0.58 mm PE tubing, Clay Adams, Sparks, MD), the chest cavity opened, and ~0.8 ml liquefied agarose (Invitrogen, Carlsbad, CA; 38 °C) was gently injected to inflate the lungs. The preparation was then placed en bloc in the refrigerator for 30 min to allow the agarose to cool and gel. The entire lung was then removed, and sliced into 300 μ m sections using a vibratome (VT1000, Leica Microsystems, Wetzlar, Germany). Slices were immersed in DMEM + Pen/Strep (Life Technologies, Carlsbad, CA) and allowed to recover overnight in an incubator (5% CO₂; 37 °C).

The following day, lung slices were rinsed in HBSS and placed in an in vitro recording chamber for live imaging of AW responses to methacholine challenge. Slices were covered with a thin lightweight sheet of mesh and a coverslip held in place with silicone grease (Molykote, Dow Corning, Midland, MI). The chamber was mounted on a microscope (DMLFS, Leica Microsystems, Wetzlar, Germany) and perfused continuously (7 ml/min) with HBSS at room temperature. A digital video camera (Rolera Fast, QImaging, Surrey, Canada) attached to the microscope was used to identify individual AWs under $\times 5$ magnification. After an initial 3 min period of baseline perfusion, slices were exposed to increasing doses of methacholine and changes in AW lumen area were recorded. The extent of AW constriction in response to increasing doses of methacholine (0.25, 0.5, 1, 2, 4, and 8 μ M; Sigma Aldrich, St Louis, MO) was determined at the end of a 2-min period of exposure at each dose. ImageJ analysis software was used to calculate the luminal area (in pixels) and the extent of AW constriction was assessed with greater decrease in lumen area interpreted as greater reactivity.

Individual AWs were chosen at random and the response to methacholine was performed on one AW/lung section, although measurements were typically collected from 1 to 2 sections per animal. Thus, treatment groups consisted typically of 1–2 AWs/animal, 2–3 animals per litter, 2–3 litters per group. AWs with a baseline area above 0.05 mm² were excluded for analysis since we showed previously they are unaffected by CPAP.¹⁰

Magnetic resonance imaging (MRI)

In a separate group of 3-day-old mice ($n = 4$), MRIs of the chest cavity were obtained for confirmation that our CPAP technique does lead to inflation of the lung rather than insufflation of the gastrointestinal systems. Individual mice were removed from the litter and placed in a customized restraint device which could be inserted into the bore of the 9.4T Bruker Biosepc small animal MRI. Unanesthetized, spontaneously breathing mice were fitted with the same mask used to deliver CPAP (see S.1), which was held in place with masking tape, inserted into the bore of the MRI, and animals allowed 2–3 min to settle before being imaged. The mask was attached to the manometer and for adjustable leak with aquarium tubing, which was then positioned next to the animal resting inside the MRI. Tubing to the mask used to control flow was extended externally to the neighboring room. Airflow to the mask was gradually increased to achieve inflation pressures of 1, 3, 6, 8, and 9 cm H₂O. A 35 mm inner diameter

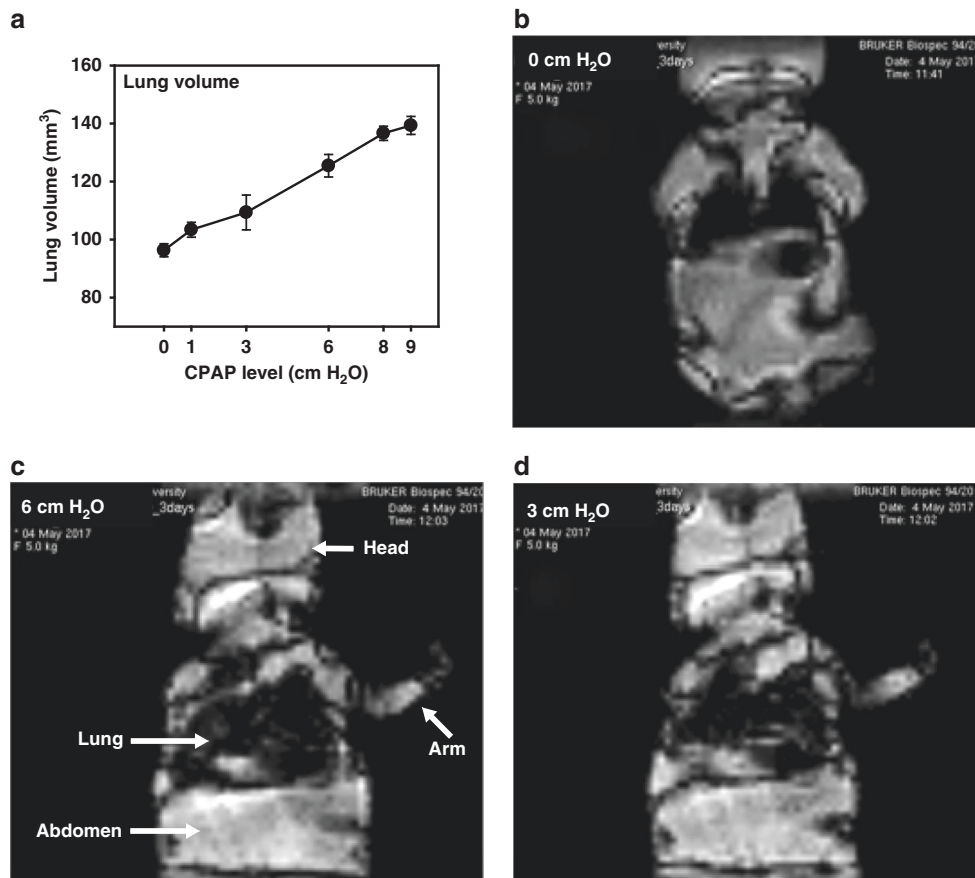


Fig. 1 CPAP-induced changes in lung volume in unanaesthetized 3-day-old mice as assessed by MRI. Mean lung volume (**a**) and representative coronal FISP MRI images of the chest cavity from a 3-day-old, spontaneously breathing mouse while on various levels of acute CPAP (**b–d**, 0, 3, and 6 cm H₂O). Values in **a** are means \pm 1 SEM. Note, for imaging purposes, lung volumes were assessed at inflation pressures up to 9 cm H₂O. For each scan, the animal was held at a given level of CPAP for \sim 60 s for image acquisition before CPAP was then increased to the next inflation pressure ($n = 4$ mice).

mouse volume coil was used to acquire all of the images. At each inflation pressure, coronal multi-slice Fast Imaging with Steady-state Free Precession (FISP) images of the chest cavity were acquired with approximately 1-s scan time. MRIs were collected from four animals, and total “lung” volume at each inflation pressure was calculated using pre-determined calibration equations. Representative MRI scans and quantification of lung volume are provided in Fig. 1.

qRT-PCR

Whole-lung tissue was removed and frozen for later analysis of mRNA expression using qRT-PCR. RNA was extracted from the frozen lung tissue using RiboZol (VWR, Radnor, PA) digestion, phenol chloroform extraction, and quantified using Nanodrop spectroscopy. cDNA was then generated using qScript cDNA synthesis kit (Quanta Biosciences) through reverse transcription. Real-time qPCR was performed with Taqman probes for HAS1–3, HYAL (1–3), *Ial*, and HA-binding protein (HABP2) CD44, TLR4, RHAMM, and TSG6 (Thermo Fischer Scientific, Waltham MA) and compared to GAPDH (Thermo Fisher) as the housekeeping gene using PerfeCTa qPCR Fastmix, UNG, ROX (Quanta Biosciences). The catalog number for PCR probes were as follows: HAS3–Mm00515009_m1; HAS1–Mm03048195_m1; CD44–Mm01277161_m1; TLR4–Mm00445273_m1; *Ial*–Mm434529_m1; RHAMM–Mm00469183_m1; TSG6–Mm00493736_m1. Duplicates were run for each sample. The fold-changes were calculated using $2^{-\Delta\Delta CT}$ method and StepOne software v2.3 (Applied Biosystems). Statistical comparisons were done using the ΔCT values.

Immunohistochemistry for HAS3 expression and α SM-actin expression

Precision-cut lung sections 150- μ m-thick were obtained from agarose inflated lungs as described above. Slices were placed in 4%

paraformaldehyde overnight. The following day, slices were stained free floating in 24-well plates by first rinsing them in phosphate-buffered saline (PBS) 3×5 min, and then incubating in blocking buffer (1% bovine serum albumin (BSA) in PBS) for 30 min at room temperature. Slices were then incubated overnight at 4 °C in HAS3 antibody (1:100; Novus Biologicals, Centennial, CO), and α SM-actin antibody directly conjugated to cy3 (1:100; Sigma Aldrich, St. Louis, MO) diluted in blocking buffer. The following day, slices were again rinsed in PBS 3×5 min, and then incubated in Donkey anti-rabbit Alexa 488 secondary antibody (1:200; Thermo Fisher Scientific, Waltham, MA) for 2 h at room temperature. The slices were rinsed in PBS 3×5 min and then stored in Vectashield mounting media (Vector Laboratories, Ontario, Canada) until imaging.

Slices were imaged for expression of HAS3 and α SM-actin around the AW using a Leica TCS SP8 confocal microscope at $\times 40$ magnification at 1024×1024 resolution. Argon and 561 diode lasers were used to image Alexa 488 and cy3 emission. To allow for a few saturated pixels, gain and offset settings of the photomultiplier were calibrated as per the manufacturer’s recommendations. A z-stack was captured for each HAS3 and α SM-actin stained AW image. All laser and gain settings were kept consistent for all images collected. No more than three AWs were imaged per lung section.

AW HAS3 and α SM-actin quantification

Image analysis was performed after loading the AW images into ImageJ and splitting the red and green channels. The background was corrected to the same level for all images. The AW was then isolated within the image. Positive staining for HAS3 was identified by adjusting the threshold equally on all images, and then quantifying the area of positive staining. The area of positive staining was then normalized to AW lumen circumference. This process was repeated for α SM-actin. For both HAS3 and α SM-actin, three z-stack images located in the center of the AW were analyzed and averaged to provide one data point per AW.

HABP immunoreactivity

At P21 mice were sacrificed by an anesthetic overdose as described above. The lungs were then inflated with a 4% paraformaldehyde solution in 0.2 M phosphate buffer supplemented with 1% cetylpyridinium chloride. Lungs were inflated at a pressure of 25 cm H₂O for 10 min with a cannula secured into the trachea, which was then tied off, and the lungs were post-fixed overnight. The lungs were then paraffin imbedded, and 5- μ m-thick sections were cut and mounted onto glass slides. For staining, slides were first deparaffinized, rehydrated in PBS for 15 min, and then incubated in blocking buffer (1% BSA in PBS) for 30 min at room temperature. Following blocking, slides were incubated for 45 min at room temperature in HABP antibody (Millipore, Burlington, MA) diluted 1:100 in blocking buffer, rinsed in PBS 3 \times 5 min, and then incubated in streptavidin conjugated Alexa 488 (1:500; Thermo Fisher Scientific, Waltham MA) for 1 h at room temperature. After staining, the slides were rinsed in PBS 3 \times 5 min and then coverslipped with Vectashield mounting media (Vector Laboratories, Ontario, Canada) until imaging. Sections were imaged on a Leica DMLP microscope (Leica Microsystems, Buffalo Grove, IL), and captured using a Qimaging Retiga EXi camera and Qcapture pro software (Teledyne photometrics, Tucson, AZ). Images were analyzed using ImageJ as described above.

FACE of glucosaminoglycans and Purple Jelly HA Assay

At P21 animals were sacrificed by overdose of anesthesia as described above. The lungs were removed, flash frozen, and stored at -80°C . FACE analysis was done as described previously.³¹ Briefly, samples were digested overnight at 60°C in proteinase K (1 mg/ml) (from Thermo Fisher Scientific, Waltham, MA), precipitated in 75% ethanol, and spun at 14,000g for 10 min twice. The resulting pellets were then resuspended in 35 μ l of 100 mM ammonium acetate and then digested with either 25 mU chondroitinase ABC (Sigma Aldrich, St. Louis, MO) or 2.5 mU Streptomyces Hyaluronidase (Sigma Aldrich, St. Louis, MO) at 37°C overnight. They were then precipitated in 100% ethanol, and spun at 14,000g for 10 min twice. The samples were lyophilized using a speed vac (Eppendorf, Vacufuge plus) at 60°C for 2–3 h under vacuum, and then rehydrated and labeled with 2-aminoacridone (AMAC; Thermo Fisher Scientific, Waltham, MA) (6.25 mM in a solution of DMSO, sodium cyanoborohydrate, and acetic acid) at 37°C for 18 h in the dark. The samples were separated on a 30% acrylamide gel at 4°C at 500 V for 1–1.5 h. The resulting gel was imaged using an Imager with UVB light (Chemidoc-it2, UVP, Upland, CA), and analyzed using ImageJ software.

The Purple Jelly Hyaluronan Assay (Biocolor, Carrickfergus, County Antrim, UK) was performed using the manufacturer's instructions. Briefly, the samples were digested in proteinase K, and the HA was precipitated and washed before mixing with the dye Stain-all. The absorbance of the dye was then read using a microplate reader (Vmax, Molecular Devices LLC, San Jose, CA) and compared to a standard curve to quantify the amount of HA present in each sample.

siRNA administration

Since HAS3 mRNA and protein expression were increased following CPAP, additional experiments were done to test whether blocking HAS3 via targeted siRNA treatment would reverse AW reactivity. Two different HAS3 siRNAs [Thermo Fisher, Waltham, MA] or scrambled siRNA [Thermo Fisher Scientific, Waltham, MA] were added to the well plates, which contained the lung slices for the respective groups. P21-day-old mice were sacrificed and lungs were prepared for measurements of AW reactivity as described above. However, immediately after lung sections were sliced using the vibrotome, individual sections of the same lung were separated between three separate wells (~3–4 slices/well) containing DMEM + Pen/strep cocktail, and each well was then randomly chosen to receive either 4 nM of siRNA, scramble siRNA, or no treatment (Ctrl). Individual slices were incubated for 48 h at 37°C in tissue culture. Incubations were repeated using a second siRNA, as well as for immunohistochemical analysis of epithelial HAS3 expression using confocal microscopy. The treatment groups included mice from both control and CPAP (i.e. 6 groups total, repeated with a second siRNA). After the incubation period, the slices were prepared for live imaging of AW responsiveness to methacholine challenge, whereas others were prepared for immunohistochemistry and confocal microscopy.

Data analysis

Statistical comparisons of responses to methacholine between control and different levels of CPAP-treated groups were made using a three-way,

repeated measures ANOVA (SigmaPlot, Systat Software Inc., San Jose, CA). Comparisons for immunohistochemistry and rtPCR between control and 6 cm H₂O CPAP were performed using a *t*-test. Differences were considered significant at $p < 0.05$. Sample sizes for animals/AWs were determined from our prior studies and subsequent power analysis.

RESULTS

MRI of neonatal mice receiving CPAP

MRI analysis was used to visualize changes in lung volume in 3-day-old, unanesthetized, spontaneously breathing mice ($n = 4$ mice). Lung volume increased with increasing inflation pressures (i.e. CPAP) up to 9 cm H₂O (Fig. 1a). Representative images of a 3-day-old mouse at progressively increasing levels of CPAP are also shown (Fig. 1b–d). These data validated our CPAP apparatus.

P21 AW reactivity to methacholine challenge

Neonatal CPAP resulted in a long-term increase in AW reactivity in both male (Fig. 2a) and female (Fig. 2b) mice, as indicated by the larger decrease in AW lumen area with increasing doses of bath-applied methacholine. In males, although a week of 1 or 3 cm H₂O CPAP tended to increase AW reactivity compared to untreated control mice, only 6 cm H₂O was statistically different from control mice. However, in females, there was a significant increase in AW reactivity with as little as 1 cm H₂O (and even greater effects with 3–6 cm H₂O). Since AW reactivity was increased in both male and female mice with 6 cm H₂O, this level of CPAP was used for the rest of the studies involving males.

Lung qrtPCR

In whole-lung homogenates, mRNA levels for enzymes involved in HA synthesis (HAS1, 2, and 3), degradation (HYAL1, 2, and 3) and several proposed signaling components (CD44, TLR4, Ial, RHAMM, and TSG6), as well as HABP2, were assessed 2 weeks after CPAP (6 cm H₂O) treatment ended (Fig. 3). CPAP-exposed lungs showed increases in HAS2 and HAS3 mRNA, whereas HAS1 was not significantly different from control mice (Fig. 3a). CPAP also increased HABP2, TLR4, RHAMM, and TSG6, whereas HYAL1, HYAL2, and HYAL3 as well as CD44, and Ial were not significantly different from control (Fig. 3b, c).

AW HAS3 and α SM-actin expression

Since CPAP (6 cm H₂O) increased lung HAS3 mRNA expression, we investigated whether it correlated with increased presence of protein using immunohistochemistry (Fig. 4). HAS3 immunoreactivity was located predominantly in AW epithelium, and its expression was increased following CPAP (Fig. 4a). Similarly, α SM-actin was also increased following CPAP (Fig. 4b), but was not notably co-localized with HAS3 (Fig. 4c, inset). Representative examples of HAS3 and α SM-actin staining are also provided (Fig. 4c).

HA quantification

Several techniques were used to quantify total HA expression in lung tissue using FACE and a commercially available ELISA-like assay of whole-lung homogenates (Fig. 5a, b), as well as immunostaining for HABP (see S2). Of all three methods used to quantify HA, none were able to detect differences between control and CPAP-treated mice. Further analysis of another glycosaminoglycan (chondroitin sulfate: 0S, 4S, 6S, and total CS (0S + 4S + 6S)) also failed to reveal a long-term effect of CPAP (Fig. 5a).

siRNA effects on AW reactivity and HAS3 expression

In P21-day-old male mice, lung slices incubated for 48 h with two different HAS3-targeted siRNAs showed reversal of CPAP-induced AW hyper-reactivity (Fig. 6a). Both siRNAs were effective, and their magnitudes of AW reactivity were similar to control-treated mice.

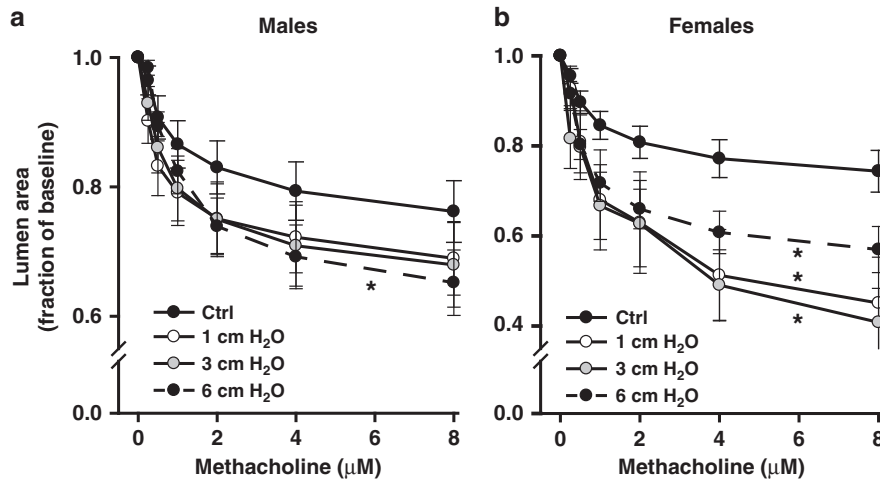


Fig. 2 Airway (AW) responses to methacholine challenge in the *in vitro* living lung slice preparation from 21-day-old mice following various levels of prior CPAP treatment. Data for males (a) and females (b) two weeks following neonatal (P1–7) CPAP. Treatment groups consist of control (Ctrl, no CPAP, solid circles/lines) and 1 (open circle), 3 (gray circle), and 6 cm H₂O (solid circle, dashed lines) CPAP. Values are expressed as the fraction of baseline lumen size. The smaller lumen size at increasing concentrations to methacholine signifies increased AW reactivity. * indicates significant difference in the slope of the response between Ctrl and CPAP animals ($N = 7\text{--}10$ airways from 4 to 5 mice/group; $*p < 0.05$ vs Ctrl).

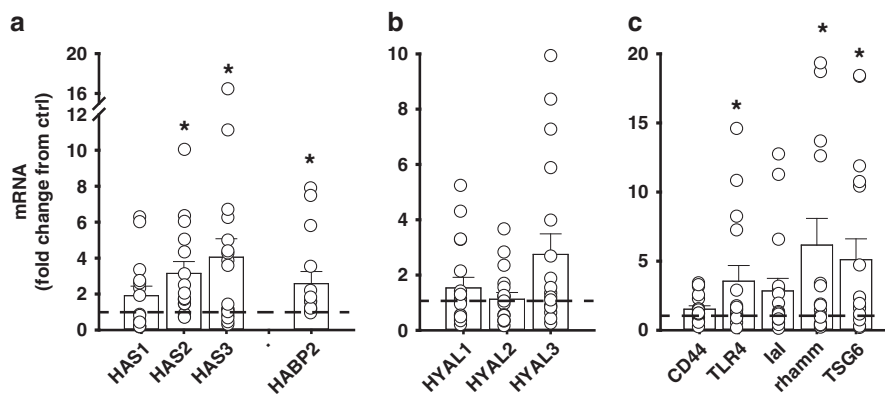


Fig. 3 Long-term (at P21 days) effects of CPAP (6 cm H₂O) on whole-lung mRNA expression. Various a hyaluronan synthases (HAS) as well as hyaluronan-binding protein-2 (HABP2), b hyaluronidases (HYAL), and c HA-associated signaling pathways. Note the increased HAS3 mRNA expression 2 weeks after CPAP treatment ended. Data are expressed as fold change from control mice. $*p < 0.05$ vs ctrl; bars are mean \pm SEM and open symbols are values from individual lungs. ($n = 15\text{--}17$ lungs/group).

Scrambled siRNA however had no effect on CPAP-exposed mice (Fig. 6a) or on the magnitude of AW reactivity of control mice who had lungs exposed to scrambled siRNA (data not shown). To confirm specificity of siRNA treatment, we randomly chose siRNA#1 to confirm successful knock-down of epithelial HAS3 expression in CPAP-treated mice (Fig. 6b). Similarly, scrambled siRNA did not affect the CPAP-induced increase in HAS3 expression. Representative images are also provided in S3.

DISCUSSION

Sex- and dose-dependent effects of CPAP on AW hyper-reactivity

The neonatal mouse model used in the current study is advantageous in terms of understanding stretch and lung distension effects on human postnatal AW development. The newborn mouse lung is at the saccular stage of development³² and comparable to an infant born prematurely at 26–28 weeks gestation. We were also able to confirm using MRI of neonatal mouse lungs that clinically relevant levels of CPAP results in lung inflation (Fig. 1). The persistence of AW hyper-reactivity in this mouse model up to 2 weeks post-CPAP treatment is translationally

relevant to the approximate timing of when wheezing manifests in former preterm infants, many of whom would likely have been on CPAP or other forms of positive pressure support while in the NICU. Similar effects on AW reactivity have been demonstrated in neonatal rats that received high intermittent positive pressure (IPP) while anesthetized daily, intubated and mechanically ventilated.³³ In our non-invasive neonatal CPAP mouse model, however, the AW hyper-reactivity likely isn't associated with significant lung injury since there was no macrophage infiltration and alveolar simplification was minimal.³⁰ In this model, however, daily lung distension alone during the early neonatal period can have long-term unintended consequences on AW development.

Our findings of persistent increased AW reactivity are relevant towards distinguishing the early effects of CPAP in prematurity for alveolar expansion and maintenance of oxygenation vs longer term detrimental effects on the bronchial AWs. However, the effects of CPAP appear to be sex-, age- and context- specific. For example, CPAP reduced AW reactivity in adult humans with asthma³⁴ and in another study in patients with sleep apnea,³⁵ suggesting CPAP may be beneficial when combined with other underlying respiratory complications. Further, in 7–8 weeks old

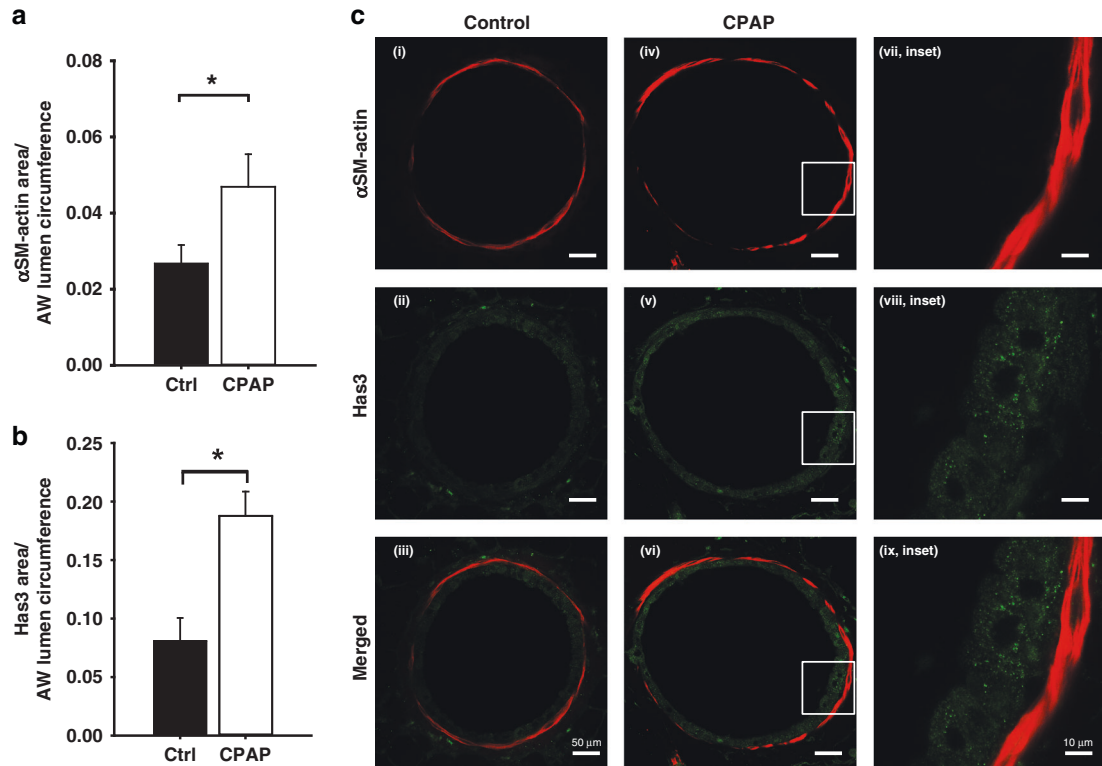


Fig. 4 CPAP effects on airway HAS3 expression. Changes in epithelial HAS3 (a) and α SM-actin (b) immunoreactivity in P21-day-old male mice, 2 weeks after CPAP (6 cm H₂O) treatment ended. Note the increase in HAS3 (a) and α SM-actin (b) immunoreactivity following CPAP. Representative images of lung sections from a control mouse (c, i–iii) and CPAP (iv–vi) treated mouse are provided, including high-resolution images (inset, vii–ix) of the white box regions from the CPAP mouse. Note, HAS3 (green) was not co-localized with airway α SM-actin (red). *Significantly different from control mice ($p < 0.05$) ($n = 8$ animals/group).

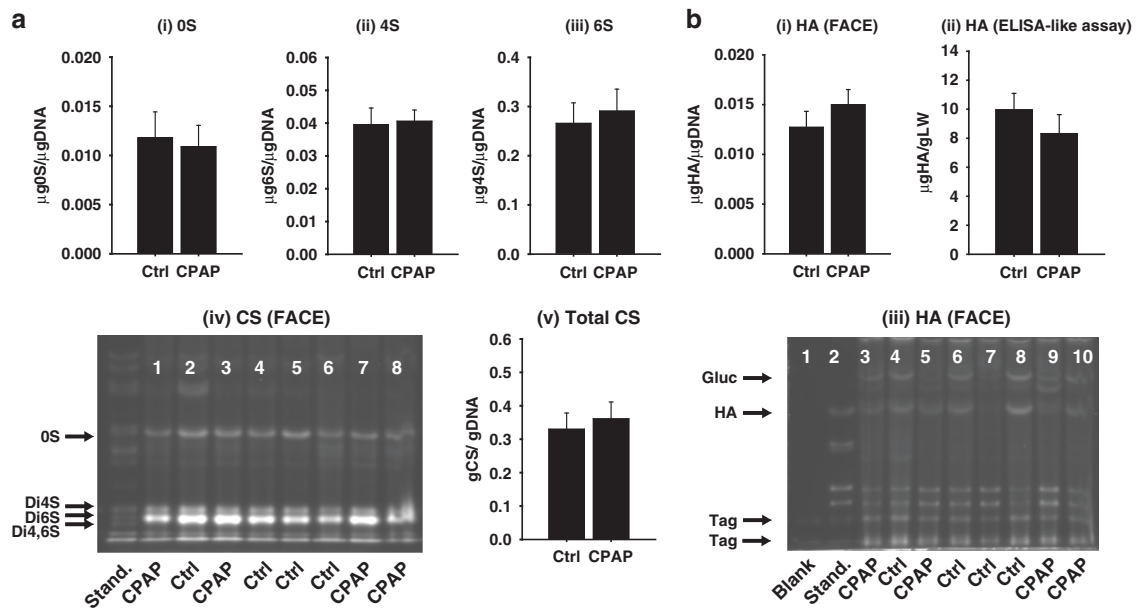


Fig. 5 CPAP effects on whole-lung HA expression. Quantification of total (a i–v) chondroitin sulfate (CS, and its constituents: 0S, 4S, and 6S) and (b i–iii) total HA using FACE (b, i) and commercially available (ELISA-like) Purple Jelly Assay (b, ii) of P21-day-old male mice. Neither total lung HA or any CS were affected by CPAP using either FACE analysis of whole-lung homogenates (a i–iv; b i,iii) or by ELISA-like assays (b ii). Representative gels are also provided (a, iv and B, iii) ($n = 10$ –12/group).

un anesthetized ferrets, continuous (24 h/day, 4 days) or nocturnal (12 h/day) CPAP reduced AW responses to acetylcholine³⁶ suggesting CPAP effects could be very different depending on the stage of lung development. In the present study, at the

highest level of CPAP (6 cm H₂O), both female and male mice were significantly hyper-reactive compared to corresponding untreated control mice, although females become more reactive at even lower levels of CPAP (1 cm H₂O) than males. Given the young age

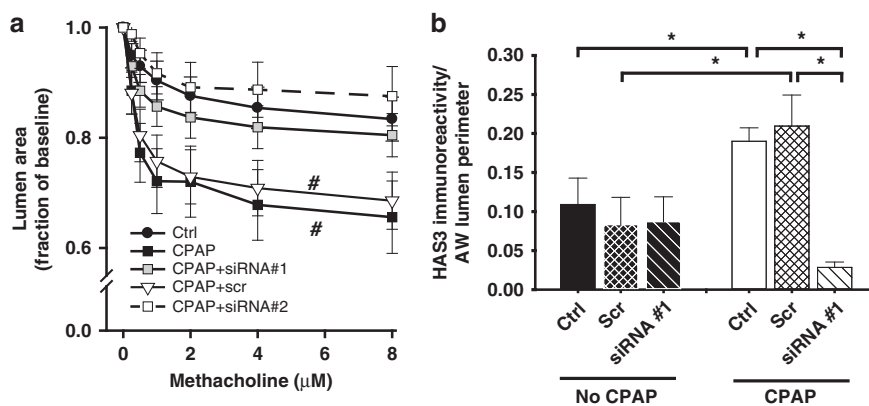


Fig. 6 Inhibition of CPAP-induced AW reactivity following HAS3 siRNA treatment. Effects of siRNA treatment on **a** CPAP-induced AW reactivity and **b** epithelial HAS3 expression in P21-day-old male mice, 2 weeks following neonatal CPAP (6 cm H₂O). Treatment groups comprise in vitro exposure (48 h incubation) of two different siRNAs targeted to HAS3 with a scrambled siRNA sequence. Note the increased AW reactivity following CPAP is reversed by siRNA treatment (**a**, siRNA#1 and #2), which was associated with decreased (vs CPAP) epithelial HAS3 expression (**b**). For clarity, scramble and siRNA data for control animal AW reactivity are not shown (**a**) and only siRNA #1 was used to show knock-down of HAS3 expression (**b**). #*p* < 0.05 in the slope of the response vs Ctrl mice. *N* = 5–6 animals per group, 2–3 AWs/animal; values means ± SEM. Representative images from **b** are shown in Fig. S3.

of the animals, it is less likely that hormonal factors per se account for these sex differences in sensitivity to CPAP, although a comprehensive exploration is beyond the scope of this study. We also previously showed sex-specific differences in the effects of CPAP during development with AW hyper-reactivity affecting males early in development (at the time of CPAP), whereas there is a delayed manifestation of AW hyper-reactivity in females.¹⁰ It was noted that earlier effects of CPAP on males implies greater sensitivity than females, although in the human infant, despite preterm boys expressing increased risk for BPD (and mechanical ventilation) while in the NICU,⁴ former preterm girls tend to exhibit a higher prevalence of respiratory morbidity as teenagers.³⁷ Collectively, these data suggest the effects of CPAP on AW reactivity are complex and likely reflect several factors including duration, intensity, and the experimental setting used to deliver pressure to the lung, as well as developmental influences. The importance of sex and the impact of respiratory support on pulmonary development should not be ignored and must be an important consideration in both animal and clinical research.

Increased AW HAS3 and αSM-actin

A notable effect of CPAP was the increased HAS3 and HABP mRNA from whole-lung homogenates. Further, AW hyper-reactivity following neonatal CPAP was associated with increased epithelial HAS3, although we were unable to confirm increased HA accumulation in lung tissue per se. This suggests that CPAP may not have affected the stable pool of constitutive HA, but does not rule out a possible effect on the rate of HA turnover via synthesis and degradation. HA is a major ECM component,^{13–15} which is synthesized via membrane-bound synthases with a significant prevalence of HA within and around AW smooth muscle, suggesting credible signaling pathways exist between HA and smooth muscle. In the present study, technical limitations prevented determination of HA size; however, since HAS3 synthesizes low molecular weight HA (<500 kDa),^{11,12,14,16} the upregulated expression of HAS3 following CPAP implies HA comprises predominantly the low MW isotype (HA_{LMW}). An inability to detect HA_{LMW} in lung tissue could suggest it is secreted into bronchial fluids. HA_{LMW} can also be formed by fragmentation of high molecular weight HA (HA^{HMW}) via hyaluronidases (HYAL),³⁸ although we did not detect significant changes in HYAL mRNA following CPAP. However, this does not necessarily rule out a role of HA_{LMW} produced by breakdown of HA^{HMW} via HYAL in the developing AWs or even with CPAP.

CPAP also caused a long-term increase in AW smooth muscle as shown by increased αSM-actin immunoreactivity. Increased ASM and metabolic activity of immature lungs stimulated by stretch³⁹ would be consistent with accelerated lung growth^{32,40} as well as exaggerated and sustained changes in ASM structure/function leading to thicker, more reactive AWs, potentially manifesting as wheezing/asthma later in life. Preterm infants that died within 32 weeks of birth exhibited significantly higher pleural HA expression, which was even higher in infants exposed to intrauterine infection.²³ Increased HA levels were associated with respiratory distress severity in a preterm primate model.²⁵ Lung HA_{LMW} expression and HAS3 mRNA are increased in mice with ventilator-induced lung injury, worsened at higher tidal volumes, but attenuated in HAS3 KO mice.¹⁷ Mice infected with RSV showed increased HA_{LMW} and Ial in BALF following subsequent chloride exposure, which was associated with increased AW reactivity.⁴¹ These data associate higher total HA, including a predominance of HA_{LMW} with perinatal lung disease, but the mechanisms by which HA acts on the target cell types are unclear. In the adult lung, HA regulates inflammation, ASM growth, and migration as well as vascular integrity and angiogenesis. Increased HA_{LMW} has been demonstrated in different pathological states, including vascular leakiness,^{42,43} cancer,^{44,45} pulmonary hypertension,⁴⁶ lung injury,^{17,18} COPD,¹⁹ asthma,^{20,21} and pulmonary fibrosis.^{18,22} Overall, there is little doubt that dysregulation of HA, particularly increased expression of HA_{LMW} is important in the pathophysiology of lung disease including that involving bronchial AWs.

The mechanisms by which HAS3 contributes to CPAP-induced AW hyper-reactivity are less clear. We expected HAS3-derived HA_{LMW} to be increased, but technical limitations impaired detection of HA size. Of interest, however, was the increased HAS3 was expressed almost exclusively in the epithelium in conjunction with increased αSM-actin, i.e., HAS3 was not co-localized with smooth muscle, which we had in fact expected. These findings suggest there may be a complex epithelial—HAS3—smooth muscle paracrine signaling mechanism underlying CPAP-induced AW hyper-reactivity. Regardless, HAS3 does appear to be important in CPAP effects given our findings that siRNA treatment reverses CPAP-induced AW hyper-reactivity, which was associated with decreased epithelial HAS3 expression. These data are consistent with findings in other conditions. Specifically, increased HAS3 mRNA has been associated with bronchial epithelial cell signaling with lung fibroblasts in asthmatic children.⁴⁷ In animal models, lung HA_{LMW} expression and HAS3 mRNA are increased in mice with ventilator-induced lung injury, which is worse at higher

tidal volumes, but attenuated in HAS3 KO mice.¹⁷ Similarly, inhibition of HAS3 blocked ventilator/sepsis-induced lung injury in vivo²⁸ and in vitro models of lung stretch.²⁹

CPAP also increased AW smooth muscle expression. Although we were unable to assess HA_{LMW}, prior studies have shown HA and or mechanical stretch of lungs can cause smooth muscle proliferation³³ and affect AW smooth muscle cell calcium signaling.^{48,49} These observations could explain the CPAP-induced AW hyper-reactivity, and increased HAS3 and smooth muscle that lasts even up to 2 weeks after CPAP treatment ended. Further studies are necessary to investigate these potential pathways in greater detail.

CONCLUSIONS

In conclusion, in our novel neonatal mouse model, we find that clinically relevant levels of CPAP cause a persistent increase in AW reactivity via an HAS3-dependent mechanism. Further work is needed to understand the mechanistic pathways contributing to the AW hyper-reactivity to determine potential longer term consequences of neonatal CPAP in preterm infants with respiratory distress syndrome. Specifically, how CPAP could contribute to the pathophysiology of lung function in the presence of other clinically relevant scenarios will be an important step forward in understanding these complex interactions, and whether HAS3 could be a viable target to treat wheezing disorders in former preterm infants.

DATA AVAILABILITY

The datasets used and/or analyzed during the current study are available from the corresponding author on reasonable request.

REFERENCES

- Baraldi, E., Carraro, S. & Filippone, M. Bronchopulmonary dysplasia: definitions and long-term respiratory outcome. *Early Hum. Dev.* **85**, 51–3 (2009).
- Jaakkola, J. J. et al. Preterm delivery and asthma: a systematic review and meta-analysis. *J. Allergy Clin. Immunol.* **118**, 823–830 (2006).
- Joshi, S. et al. Exercise-induced bronchoconstriction in school-aged children who had chronic lung disease in infancy. *J. Pediatr.* **162**, 813–818 e811 (2013).
- Laughon, M. M. et al. Prediction of bronchopulmonary dysplasia by postnatal age in extremely premature infants. *Am. J. Respir. Crit. Care Med.* **183**, 1715–1722 (2011).
- Belik, J., Jankov, R. P., Pan, J. & Tanswell, A. K. Chronic O₂ exposure enhances vascular and airway smooth muscle contraction in the newborn but not adult rat. *J. Appl. Physiol.* **94**, 2303–2312 (2003).
- Denis, D. et al. Prolonged moderate hyperoxia induces hyperresponsiveness and airway inflammation in newborn rats. *Pediatr. Res.* **50**, 515–519 (2001).
- Hershenson, M. B. et al. Recovery of airway structure and function after hyperoxic exposure in immature rats. *Am. J. Respir. Crit. Care Med.* **149**, 1663–1669 (1994).
- O'Reilly, M. & Thebaud, B. Animal models of bronchopulmonary dysplasia. The term rat models. *Am. J. Physiol. Lung Cell. Mol. Physiol.* **307**, L948–958 (2014).
- Wang, H. et al. Severity of neonatal hyperoxia determines structural and functional changes in developing mouse airway. *Am. J. Physiol. Lung Cell Mol. Physiol.* **307**, L295–301 (2014).
- Mayer, C. A., Martin, R. J. & MacFarlane, P. M. Increased airway reactivity in a neonatal mouse model of continuous positive airway pressure. *Pediatr. Res.* **78**, 145–151 (2015).
- Cyphert, J. M., Trempus, C. S. & Garantziotis, S. Size matters: molecular weight specificity of hyaluronan effects in cell biology. *Int. J. Cell Biol.* **2015**, 563818 (2015).
- Garantziotis, S., Brezina, M., Castelnuovo, P. & Drago, L. The role of hyaluronan in the pathobiology and treatment of respiratory disease. *Am. J. Physiol. Lung Cell. Mol. Physiol.* **310**, L785–795 (2016).
- Jiang, D., Liang, J. & Noble, P. W. Hyaluronan as an immune regulator in human diseases. *Physiol. Rev.* **91**, 221–264 (2011).
- Lauer, M. E., Dweik, R. A., Garantziotis, S. & Aronica, M. A. The rise and fall of hyaluronan in respiratory diseases. *Int. J. Cell Biol.* **2015**, 712507 (2015).
- Vigetti, D. et al. Hyaluronan: biosynthesis and signaling. *Biochim. Biophys. Acta* **1840**, 2452–2459 (2014).
- Wang, A., de la Motte, C., Lauer, M. & Hascall, V. Hyaluronan matrices in pathobiological processes. *FEBS J.* **278**, 1412–1418 (2011).
- Bai, K. J. et al. The role of hyaluronan synthase 3 in ventilator-induced lung injury. *Am. J. Respir. Crit. Care Med.* **172**, 92–98 (2005).
- Garantziotis, S. et al. Serum inter-alpha-trypsin inhibitor and matrix hyaluronan promote angiogenesis in fibrotic lung injury. *Am. J. Respir. Crit. Care Med.* **178**, 939–947 (2008).
- Dentener, M. A., Vernooy, J. H., Hendriks, S. & Wouters, E. F. Enhanced levels of hyaluronan in lungs of patients with COPD: relationship with lung function and local inflammation. *Thorax* **60**, 114–119 (2005).
- Liang, J. et al. Role of hyaluronan and hyaluronan-binding proteins in human asthma. *J. Allergy Clin. Immunol.* **128**, 403–411 e403 (2011).
- Vignola, A. M. et al. Airway inflammation in mild intermittent and in persistent asthma. *Am. J. Respir. Crit. Care Med.* **157**, 403–409 (1998).
- Bjerner, L., Lundgren, R. & Hallgren, R. Hyaluronan and type III procollagen peptide concentrations in bronchoalveolar lavage fluid in idiopathic pulmonary fibrosis. *Thorax* **44**, 126–131 (1989).
- Johnsson, H., Eriksson, L., Gerdin, B., Hallgren, R. & Sedin, G. Hyaluronan in the human neonatal lung: association with gestational age and other perinatal factors. *Biol. Neonate* **84**, 194–201 (2003).
- Johnsson, H., Eriksson, L., Jonzon, A., Laurent, T. C. & Sedin, G. Lung hyaluronan and water content in preterm and term rabbit pups exposed to oxygen or air. *Pediatr. Res.* **44**, 716–722 (1998).
- Juul, S. E. et al. Changes in hyaluronan deposition during early respiratory distress syndrome in premature monkeys. *Pediatr. Res.* **35**, 238–243 (1994).
- Wang, P. M. & Lai-Fook, S. J. Effects of ventilation on hyaluronan and protein concentration in pleural liquid of anesthetized and conscious rabbits. *Lung* **176**, 309–324 (1998).
- Wang, P. M. & Lai-Fook, S. J. Pleural tissue hyaluronan produced by postmortem ventilation in rabbits. *Lung* **178**, 1–12 (2000).
- Mrabat, H. et al. Inhibition of HA synthase 3 mRNA expression, with a phosphodiesterase 3 inhibitor, blocks lung injury in a septic ventilated rat model. *Lung* **187**, 233–239 (2009).
- Mascarenhas, M. M. et al. Low molecular weight hyaluronan from stretched lung enhances interleukin-8 expression. *Am. J. Respir. Cell Mol. Biol.* **30**, 51–60 (2004).
- Reyburn, B. et al. The effect of continuous positive airway pressure in a mouse model of hyperoxic neonatal lung injury. *Neonatology* **109**, 6–13 (2016).
- Calabro, A., Benavides, M., Tammi, M., Hascall, V. C. & Midura, R. J. Microanalysis of enzyme digests of hyaluronan and chondroitin/dermatan sulfate by fluorophore-assisted carbohydrate electrophoresis (FACE). *Glycobiology* **10**, 273–281 (2000).
- Backstrom, E., Hogmalm, A., Lappalainen, U. & Bry, K. Developmental stage is a major determinant of lung injury in a murine model of bronchopulmonary dysplasia. *Pediatr. Res.* **69**, 312–318 (2011).
- Fukunaga, T., Davies, P., Zhang, L., Hashida, Y. & Motoyama, E. K. Prolonged high intermittent positive-pressure ventilation induces airway remodeling and reactivity in young rats. *Am. J. Physiol.* **275**, L567–573 (1998).
- Busk, M. et al. Use of continuous positive airway pressure reduces airway reactivity in adults with asthma. *Eur. Respir. J.* **41**, 317–322 (2013).
- Nandwani, N., Caranza, R. & Hanning, C. D. Obstructive sleep apnoea and upper airway reactivity. *J. Sleep. Res.* **7**, 115–118 (1998).
- Xue, Z., Yu, Y., Gao, H., Gunst, S. J. & Tepper, R. S. Chronic continuous positive airway pressure (CPAP) reduces airway reactivity in vivo in an allergen-induced rabbit model of asthma. *J. Appl. Physiol.* **111**, 353–357 (2011).
- Vrijlandt, E. J., Gerritsen, J., Boezen, H. M. & Duiverman, E. J. Gender differences in respiratory symptoms in 19-year-old adults born preterm. *Respir. Res.* **6**, 117 (2005).
- Stern, R., Asari, A. A. & Sugahara, K. N. Hyaluronan fragments: an information-rich system. *Eur. J. Cell Biol.* **85**, 699–715 (2006).
- Liu, M. et al. Stimulation of fetal rat lung cell proliferation in vitro by mechanical stretch. *Am. J. Physiol.* **263**, L376–383 (1992).
- Zhang, S., Garbutt, V. & McBride, J. T. Strain-induced growth of the immature lung. *J. Appl. Physiol.* (1985) **81**, 1471–1476 (1996).
- Song, W. et al. Respiratory syncytial virus infection increases chlorine-induced airway hyperresponsiveness. *Am. J. Physiol. Lung Cell Mol. Physiol.* **309**, L205–210 (2015).
- Etscheid, M., Kress, J., Seitz, R. & Dodt, J. The hyaluronic acid-binding protease: a novel vascular and inflammatory mediator? *Int. Immunopharmacol.* **8**, 166–170 (2008).
- Singleton, P. A. et al. High-molecular-weight hyaluronan is a novel inhibitor of pulmonary vascular leakiness. *Am. J. Physiol. Lung Cell. Mol. Physiol.* **299**, L639–651 (2010).
- Liu, N. et al. Hyaluronan synthase 3 overexpression promotes the growth of TSU prostate cancer cells. *Cancer Res.* **61**, 5207–5214 (2001).
- Rangel, M. P. et al. Tissue hyaluronan expression, as reflected in the sputum of lung cancer patients, is an indicator of malignancy. *Braz. J. Med. Biol. Res.* **48**, 557–567 (2015).
- Aytekin, M. et al. High levels of hyaluronan in idiopathic pulmonary arterial hypertension. *Am. J. Physiol. Lung Cell. Mol. Physiol.* **295**, L789–799 (2008).

47. Reeves, S. R. et al. Asthmatic bronchial epithelial cells promote the establishment of a Hyaluronan-enriched, leukocyte-adhesive extracellular matrix by lung fibroblasts. *Respir. Res.* **19**, 146 (2018).
48. Lazrak, A. et al. Hyaluronan mediates airway hyperresponsiveness in oxidative lung injury. *Am. J. Physiol. Lung Cell Mol. Physiol.* **308**, L891–903 (2015).
49. Lazrak, A. et al. Upregulation of airway smooth muscle calcium-sensing receptor by low-molecular-weight hyaluronan. *Am. J. Physiol. Lung Cell Mol. Physiol.* **318**, L459–L471 (2020).

ACKNOWLEDGEMENTS

We would like to acknowledge the commitment from Morgan Hazard for assistance with CPAP exposure.

AUTHOR CONTRIBUTIONS

C.A.M., A.G., A.M., V.C. and P.M.M. made substantial contributions to data acquisition and analysis; C.A.F. and B.O.E. performed MRIs; V.C.H. and R.J.Midura. provided technical and data interpretation expertise; P.M.M., C.M.P., Y.S.P. and R.J.Martin. contributed to conception and experimental design. P.M.M. drafted the manuscript and all authors revised it critically for intellectual content and approval of the submitted and final version.

FUNDING INFORMATION

This work was funded by the National Heart, Lung and Blood Institute (Bethesda, MD) Grants R01HL138402 (P.M.M. and C.M.P.), R01HL056470 (Y.S.P. and R.J.Martin.),

NIH grant S10-OD024996, NHLBI PO1HL107147 and the Department of Pediatrics, Rainbow Babies and Children's Hospital, Cleveland, Ohio. This study was also funded in part by generous financial contributions from William and Lois Briggs.

COMPETING INTERESTS

The authors declare no competing interests.

ETHICS APPROVAL

All procedures were carried out in accordance with the National Institute of Health (NIH) guidelines for care and use of laboratory animals and were approved by the Animal Care and Use Committee at Case Western Reserve University.

ADDITIONAL INFORMATION

Supplementary information The online version contains supplementary material available at <https://doi.org/10.1038/s41390-021-01695-0>.

Correspondence and requests for materials should be addressed to PeterM. MacFarlane

Reprints and permission information is available at <http://www.nature.com/reprints>

Publisher's note Springer Nature remains neutral with regard to jurisdictional claims in published maps and institutional affiliations.